Deterministic synthesis of mechanical NOON states in ultrastrong optomechanics

V. Macrí, L. Garziano, A. Ridolfo, O. Di Stefano, and S. Savasta
Dipartimento di Fisica e di Scienze Terra Terra, Università di Messina, Viale F. Stagno d'Alcontres 31, I-98166 Messina, Italy
(Received 18 May 2016; published 8 July 2016)

We propose a protocol for the deterministic preparation of entangled NOON mechanical states. The system is constituted by two identical, optically coupled optomechanical systems. The protocol consists of two steps. In the first, one of the two optical resonators is excited by a resonant external π-like Gaussian optical pulse. When the optical excitation coherently partly transfers to the second cavity, the second step starts. It consists of sending simultaneously two additional π-like Gaussian optical pulses, one at each optical resonator, with specific frequencies. In the optomechanical ultrastrong coupling regime, when the coupling strength becomes a significant fraction of the mechanical frequency, we show that NOON mechanical states with quite high Fock states can be deterministically obtained. The operating range of this protocol is carefully analyzed. Calculations have been carried out taking into account the presence of decoherence, thermal noise, and imperfect cooling.

DOI: 10.1103/PhysRevA.94.013817

I. INTRODUCTION

Cavity optomechanics studies optical cavities and mechanical resonators interacting via radiation pressure and mechanical back-action. The manipulation and detection of mechanical motion in the quantum regime using radiation pressure is promising for applications in quantum information processing [1,2], where optomechanical devices could serve as coherent light-matter interfaces which may allow for storage of quantum information in long-lived phonon states [3]. Specifically, hybrid systems, consisting of electromagnetic resonators and mechanical oscillators constitute a promising platform for realizing quantum memory or quantum state transfer among different nodes of a quantum network [4–7].

Mechanical oscillators in the quantum regime are also systems with great potential in sensing and quantum metrology [8–15]. Moreover, they could offer a route to new tests of quantum theory at unprecedented size and mass scales. These experiments could help the understanding of decoherence processes in massive objects. These systems are promising as a means to control and observe quantum superpositions of macroscopic objects [16–18]. The optomechanical interaction can also be exploited to create interesting quantum states in both the optical and the mechanical subsystems and to create entangled states between the two subsystems or between different mechanical systems. One of the most straightforward applications of quantum optomechanics, regarding the manipulation of the photon quantum states, consists of squeezing the noise of the light beam [19–21]. A review of the current efforts toward demonstrating shot-noise effects and squeezing in optomechanical experiments can be found in Ref. [22]. The realizations of cavity optomechanical systems with both atomic clouds and photonic crystal cavities have allowed the demonstration of mechanical-induced optical squeezing at the quantum level [23,24].

The generation of nonclassical mechanical states requires cooling of the system to its ground state. Experimentally, ground-state cooling with conventional cryogenics can be reached only for high-frequency mechanical oscillators. The first demonstration of quantum control at the single-phonon level was demonstrated with a ∼6-GHz piezoelectric mechanical oscillator cooled below 50 mK [25]. For lower-frequency mechanical oscillators, ground-state cooling can be obtained by combining cryogenic precooling with dynamical back-action laser cooling. Optical feedback cooling based on the radiation pressure force was demonstrated in the vibrational modes of a macroscopic end-mirror [26]. Radiation-pressure cavity cooling, for suspended micromirrors [27] and for microtoroids [28], has also been demonstrated. It has been shown that, starting from the system ground state, it is possible, in principle, to synthesize arbitrary mechanical quantum states in a completely controlled and deterministic manner [29]. The general strategy for creating such states was described by Law and Eberly in the context of cavity QED [30]. Quantum state engineering of the electromagnetic field of an optical mode has been demonstrated in the context of cavity quantum electrodynamics and in circuit quantum electrodynamics [31–34]. The approach by Xu *et al.* [29] applies to optomechanical systems the protocols developed for the synthesis of arbitrary motional states of a trapped ion [35–37], inspired by the Law and Eberly protocol [30]. Recently, Garziano *et al.* proposed a different cavity-optomechanics protocol working in the ultrastrong-coupling (USC) regime, which in a single step forces the ground state of a mechanical oscillator to evolve into the target quantum state in a completely controlled and deterministic manner, the only limitation being the strength of the optomechanics interaction [38].

The classification of the different interaction regimes based on the interaction strength is not universal. In analogy with cavity QED, the USC regime can be referred to as the regime where the coupling strength g_M becomes comparable to the transition frequency of the mechanical resonator ω_M [38]. This regime is also known as beyond Lamb-Dicke [37,39]. The regime where the radiation pressure of a single photon displaces the mechanical resonator by more than its zero-point uncertainty, corresponding to $g_M \geqslant \omega_M$, has been designated as the single-photon strong-coupling regime [40]. Optomechanics experiments are rapidly approaching the USC regime [11]. Achieving it in optomechanical systems will facilitate the creation of quantum mechanical states of the mechanical resonator, as well as the characterization of such states by measuring the cavity photon field [40–42]. USC is

 ©2016 American Physical Society

attracting great interest also in cavity QED because it can give rise to novel quantum effects [43–49].

In the single-photon strong-coupling regime, it has been shown that, starting from a superposition of photon states inside the cavity, it is possible to create a Schrödinger cat-type state, where a microscopic degree of freedom (the optical cavity mode) is entangled with a "macroscopic" degree of freedom (the vibrating mirror) [31,50,51]. Experimental schemes for obtaining entanglement between mechanical motion and the optical cavity have also been analyzed for the continuous-variable case [52,53]. Recently, it has been shown that a suitable time-dependent modulation of the drive can improve the efficiency of photon-phonon entanglement [54].

Several different protocols and techniques have been proposed in order to create entanglement of spatially separated mechanical oscillators, exploiting radiation pressure [55,56]. A heralded probabilistic scheme, working in the optomechanical USC regime, to generate mechanical NOON states [57,58] with arbitrary phonon numbers by measuring the sideband photons has been proposed [59]. Using sideband excitations, it has been shown that arbitrary entangled states of vibrational modes of different membranes embedded inside a cavity can be produced in principle by sequentially applying a series of classical pulses with specific frequencies, phases, and durations [39]. In the case of two mechanical resonators coupled to the same driven cavity mode, a realistic protocol for the heralded preparation and readout of mechanical Bell states has been proposed [60,61]. A scheme to transfer continuous variable entanglement from the squeezed light to the mechanical motion of movable mirrors has been recently proposed [62].

Here we propose a protocol for the deterministic preparation of entangled NOON states or even more general mechanical states between two identical, optically coupled optomechanical systems. Two key features of this scheme are the following: (i) entanglement can be generated with a few steps independently of the highest phonon number present in the entangled state, and (ii) the protocol is deterministic. This approach extends a recently proposed scheme for a single-step arbitrary control of mechanical quantum states in a single optomechanical system in the USC regime [38]. The system here studied has already been proposed to generate quantum entanglement between two mechanical resonators involving zero- and one-phonon states [63], by considering a large photon hopping regime. The protocol here presented is an example of how the USC regime can favor the generation and control of mechanical quantum entangled states.

II. MODEL

We start by considering two identical, optically coupled optomechanical systems (see Fig. 1). We mainly focus on the USC regime, although we also present results obtained for lower coupling rates.

The total Hamiltonian of the system is ($\hbar = 1$)

$$\hat{H}_S = \sum_{i=1}^{2} \hat{H}_0^{(i)} + \hat{H}_I, \tag{1}$$

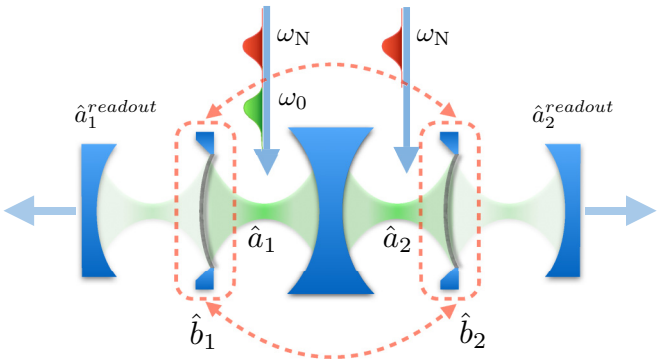

FIG. 1. Schematic setup of two identical optically coupled optomechanical systems. Each mechanical oscillator, with frequency ω_M, is parametrically coupled with a single-mode optical resonator and/or cavity, which can be driven by external π-like Gaussian optical pulses with specific central frequencies. One cavity mirror can be added to the end of both the optomechanical systems for optical readout.

where

$$\hat{H}_0^{(i)} = \omega_R \hat{a}_i^\dagger \hat{a}_i + \omega_M \hat{b}_i^\dagger \hat{b}_i + g_M \hat{a}_i^\dagger \hat{a}_i (\hat{b}_i + \hat{b}_i^\dagger) \tag{2}$$

describes the two uncoupled optomechanical systems and

$$\hat{H}_I = g_R (\hat{a}_1^\dagger \hat{a}_2 + \hat{a}_1 \hat{a}_2^\dagger) \tag{3}$$

describes their optical coupling, where g_R is the coupling rate between the two optical resonators. In Eq. (2), ω_R is the resonance frequency of the optical resonator, ω_M is the mechanical resonance frequency, and $g_M = \omega_R' x_{\mathrm{ZPF}}$ is the optomechanical coupling. Here $x_{\mathrm{ZPF}} = (2\mathcal{M}\omega_M)^{-1/2}$, representing the zero-point uncertainty, where $\mathcal{M}$ is the mass of the mechanical oscillator and ω_M' is the derivative of the resonator energy with respect to the mechanical oscillator position. The operators $\hat{a}_i$ and $\hat{b}_i$ are, respectively, the standard Bosonic annihilation operators for the ith cavity mode and the mechanical oscillator. In Eq. (3), the counter-rotating terms proportional to $\hat{a}_1^\dagger \hat{a}_2^\dagger$ and $\hat{a}_1 \hat{a}_2$ have been dropped, owing to the smallness of the coupling strength between the two optical resonators, with respect to their resonance frequency, considered in this work.

The two optomechanical systems interact only via optical coupling. When $g_R = 0$, i.e., there is no interaction between the two cavities, each Hamiltonian in Eq. (2) conserves its photon number ($[\hat{a}_i^\dagger \hat{a}_i, \hat{H}_0^{(i)}] = 0$), and it can be diagonalized separately. In each n-photonic Fock subspace, the Hamiltonian describes a harmonic oscillator with frequency ω_M which is displaced by $-n x_0$, where $x_0 = 2 x_{\mathrm{ZPF}}\, g_M^2/\omega_M$ is the displacement caused by a single photon. The eigenvalues of the Hamiltonian in Eq. (2) are $E_{nm}^{(i)} = n\omega_R - \frac{n^2 g_M^2}{\omega_M} + m\omega_M$, and the corresponding eigenstates can be expressed as

$$|n,m\rangle_i = |n\rangle_i e^{n\beta_0 (\hat{b}_i^\dagger - \hat{b}_i)} |m\rangle_i, \tag{4}$$

where $\beta_0 = g_M/\omega_M$ and $|m\rangle_i = (1/\sqrt{m!})(b_i^\dagger)^m |0\rangle_i$. The $|1,0\rangle_i$ state represents the mechanical ground state of the $n = 1$ manifold displaced harmonic oscillator. It corresponds to a mechanical coherent state that can be expanded in terms of the

bare mechanical states $|m\rangle_i$ with the well-known expression

$$|1,0\rangle_i = |1\rangle_i \sum_{m=0}^{\infty} d_m |m\rangle_i, \tag{5}$$

with

$$d_m = \frac{(-\beta_0)^m}{\sqrt{m!}} e^{-\frac{1}{2}\beta_0^2}. \tag{6}$$

If $g_R = 0$, the eigenstates of the Hamiltonian in Eq. (1) can be written as

$$|n_1,m_1,n_2,m_2\rangle = |n_1,m_1\rangle_1 \otimes |n_2,m_2\rangle_2, \tag{7}$$

where the integers n_i and m_i represent, respectively, the number of photons and vibrational excitation in the ith optomechanical system.

III. THE PROTOCOL

We first describe the two-step protocol for the *deterministic* preparation of mechanical entangled NOON states:

$$|\bar{\psi}\rangle = \alpha|0,N,0,0\rangle + \beta e^{i\varphi}|0,0,0,N\rangle, \quad \alpha,\beta \in \mathbb{R}^+. \tag{8}$$

We consider that the two optical cavities are interacting ($g_R \neq 0$), and the system is initially prepared in its ground state $|0,0,0,0\rangle$ (no photons in the cavities and the mechanical oscillators are in their ground state). We neglect the coupling of the system with its environment, in this initial presentation, in order to focus on the key points of the protocol. The influence of pulse width and transition matrix elements on the achievement of the target quantum state is discussed below under the subsection "Operating limits."

The first step consists of the excitation of one of the two optical resonators (e.g., resonator 1) by an external π-like Gaussian optical pulse resonant with the transition $|0,0,0,0\rangle \leftrightarrow |1,m,0,0\rangle$ (pulse 1). Since the system is totally symmetrical, results do not change if we apply pulse 1 to either cavity 1 or cavity 2. In the following we consider the case where pulse 1 is sent to cavity 1. In the regimes here investigated, where the optomechanical coupling induces the photon blockade, the resulting state is $|1,m,0,0\rangle$. For $g_R \neq 0$ this state is not an eigenstate of the Hamiltonian in Eq. (1). As a consequence, the system will undergo Rabi-like oscillations and the time evolution of the state of the system will be given by

$$|\psi(t)\rangle = \cos(g_R t)|1,m,0,0\rangle - i\sin(g_R t)|0,0,1,m\rangle. \tag{9}$$

This energy exchange between the two resonators can be interrupted by sending simultaneously two additional optical π pulses, (pulses 2 and 3, one exciting each cavity) resonant with the transition $|1,m\rangle_i \rightarrow |0,N\rangle_i$ (step 2). If we want to create a NOON state with specific probability amplitudes $\beta = \sin(g_R t^*)$, $\alpha = \cos(g_R t^*)$, these two additional optical pulses must be sent at $t^* = g_R^{-1}\arctan(\beta/\alpha)$. A key point is that the ket $|0,0\rangle_i$ will remain unchanged after the arrival of such pulses, because the central frequency of the pulse is very far from the transition frequency of $|0,0\rangle_i \rightarrow |1,0\rangle_i$ as schematically shown in Fig. 2. This will produce the desired entangled mechanical state. If the two optical pulses have the same phase, the following state is obtained,

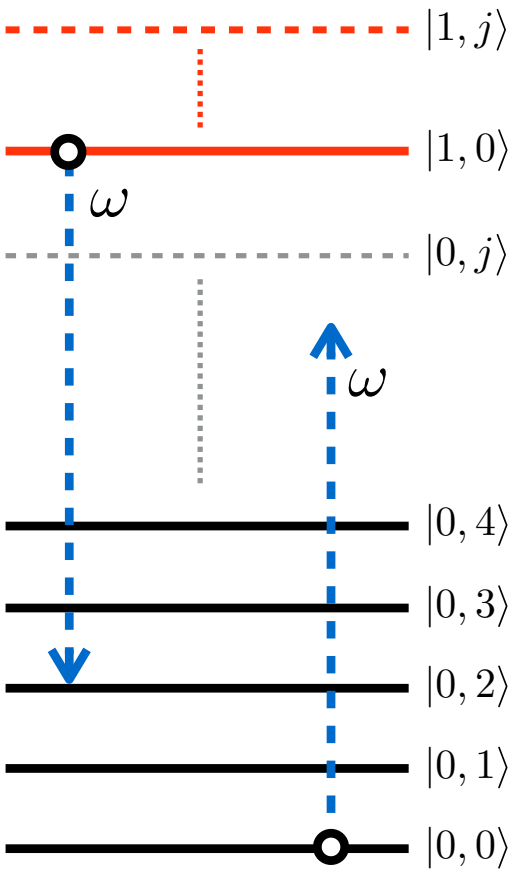

FIG. 2. Scheme of the lowest energy levels for a single optomechanical system. If the system is in the state $|1,0\rangle$, a resonant optical π pulse, described by the blue arrow, induces the transition $|1,0\rangle \rightarrow |0,2\rangle$. If the system is in the state $|0,0\rangle$, no transitions can be induced by the same pulse.

$$|\bar{\psi}\rangle = \alpha\,|0,N,0,0\rangle - i\beta\,|0,0,0,N\rangle, \tag{10}$$

which, dropping the factorized photonic kets, can be also written as

$$|\bar{\psi}\rangle_{\rm mech} = \alpha\,|N,0\rangle_{\rm mech} - i\beta\,|0,N\rangle_{\rm mech}. \tag{11}$$

The highest mechanical number state N that can be obtained in this NOON state strongly depends on the normalized mechanical coupling strength β_0.

We now proceed to a more detailed description of the protocol. The total system Hamiltonian in the presence of the input optical pulses (dissipation and decoherence effects are described later by the master equation approach) reads

$$\hat{H} = \hat{H}_S + \hat{H}_d^{(0)}(t) + \sum_{i=1}^{2} \hat{H}_d^{(i)}(t), \tag{12}$$

where

$$\hat{H}_d^{(0)}(t) = \mathcal{E}_0(t)\cos(\omega_0 t)\hat{X}_1 \tag{13}$$

describes the external driving pulse 1 (first step), with $\mathcal{E}_0(t) = \sqrt{\kappa}\,A_0\,\mathcal{G}_\Delta(t - t_0)$. Here, A_0 is the pulse

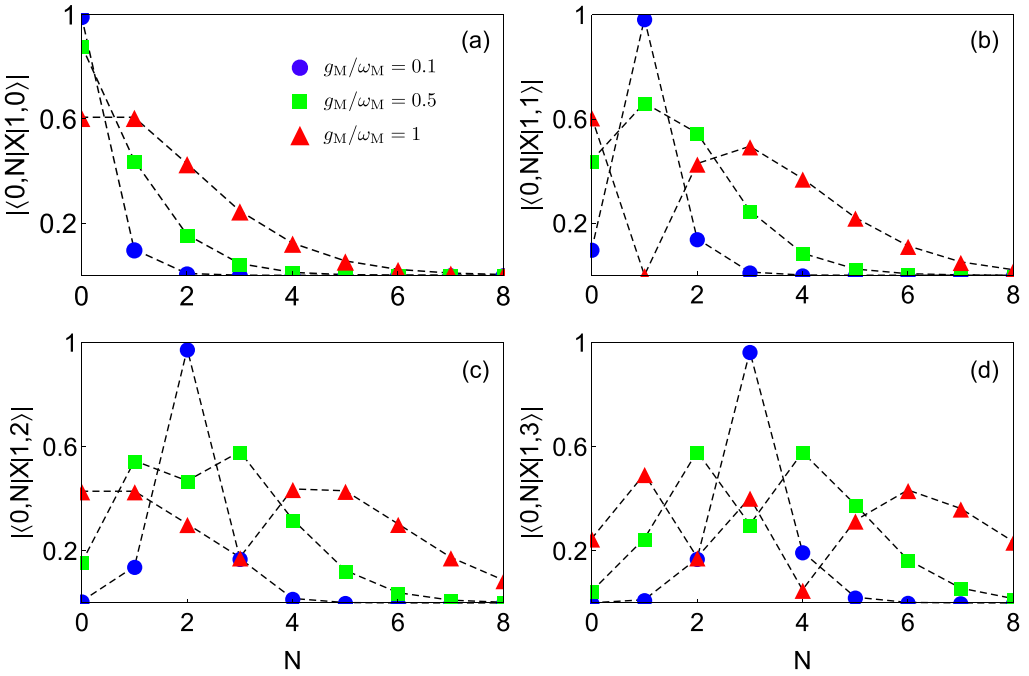

FIG. 3. Transition matrix elements $\langle 0,N|\hat{X}|1,m\rangle$ between the intermediate state $|1,m\rangle$ and the mechanical state $|0,N\rangle$ as a function of the vibrational quantum number N for different values of the optomechanical coupling rates $g_M/\omega_M = 0.1$ (blue solid circles), $g_M/\omega_M = 0.5$ (green solid squares), and $g_M/\omega_M = 1$ (red solid triangles), when the ancilla state has phonon numbers (a) $m = 0$, (b) $m = 1$, (c) $m = 2$, and (d) $m = 3$.

amplitude, κ is the cavity damping rate, and $\mathcal{G}_\Delta(t-t_0) = \exp[-(t-t_0)^2/(2\Delta^2)]/(\Delta\sqrt{2\pi})$ is a normalized Gaussian function describing the pulse shape. Moreover, $\hat{X}_1 = \hat{a}_1^\dagger + \hat{a}_1$ and $\omega_0 = E_{1m} - E_{00}$ is the energy gap between the *ancilla* state $|1,m,0,0\rangle$ and the ground state $|0,0,0,0\rangle$. We now move to the frame that diagonalizes the system Hamiltonian $\hat{H}_S$ by expressing the driving Hamiltonian in the dressed basis of the system energy eigenstates, and we can focus our attention on the case in which the driving fields are resonant with the transitions $|1,m,0,0\rangle \leftrightarrow |0,0,0,0\rangle$. In the interaction picture (with respect to $\hat{H}_S$) and neglecting the nonresonant time-oscillating terms, $\hat{H}_d^{(0)}$ reduces to the following effective driving Hamiltonian:

$$\hat{H}_{\rm eff}^{(0)} = \mathcal{E}_m(t)|0,0,0,0\rangle\langle 1,m,0,0| + \text{H.c.}, \tag{14}$$

where the effective amplitude $\mathcal{E}_m(t)$ of the driving field is given by

$$\mathcal{E}_m(t) = \frac{\mathcal{E}_0(t)}{2}\langle 0,0,0,0|\hat{X}_1|1,m,0,0\rangle. \tag{15}$$

The necessary and sufficient condition to ensure that the *ancilla* state is completely populated by external drive pulse is $\int_{-\infty}^{\infty}|\mathcal{E}_m(t)|dt = \pi$. This condition is fulfilled if $A_0\sqrt{\kappa}|\langle 0,0,0,0|\hat{X}_{(1)}|1,m,0,0\rangle| = \pi$. As described above, since the two cavities are optically coupled, after the arrival of the first pulse at cavity 1, the excitation spontaneously transfers towards the second cavity, and the resulting state is the superposition in Eq. (9).

The last term in Eq. (12) describes the equal (except for a possible phase factor) external driving pulses that are sent to both the cavities in the second step. The driving Hamiltonian $\hat{H}_d^{(i)}$ corresponding to excitation of the ith cavity can be expressed as

$$\hat{H}_d^{(i)} = \sum_{j=1}^{k}\mathcal{E}_j(t)\cos\left(\omega_j t + \eta_j^{(i)}\right)\hat{X}_i. \tag{16}$$

In order to depopulate the intermediate ancilla state $|1,m\rangle_i$ towards the $|0,m'\rangle_i$ states, two optical π-like pulses at both cavities have to be sent, at the same instant of time t^*. Then, the target NOON state $|\bar{\psi}\rangle$, in Eq. (8), can be obtained by sending, at each cavity, one quasimonochromatic optical pulse with central frequency $\omega_N = E_{1m} - E_{0N}$. Following the above-described procedure, $\hat{H}_d^{(1)}$ can be approximated by the effective driving Hamiltonian:

$$\hat{H}_{\rm eff}^{(1)} = \mathcal{E}_{m,N}(t)e^{i\eta_N^{(1)}}|0,N,0,0\rangle\langle 1,m,0,0| + \text{H.c.}, \tag{17}$$

where the effective amplitudes $\mathcal{E}_{m,N}(t)$ of the driving fields are given by

$$\mathcal{E}_{m,N}(t) = \frac{\mathcal{E}_1(t)}{2}\langle 0,N,0,0|\hat{X}_1|1,m,0,0\rangle, \tag{18}$$

with $\mathcal{E}_1(t) = \sqrt{\kappa}A_1\mathcal{G}_\Delta(t-t_1)$. In this case, the complete transfer of the excitation from the ancilla states to the mechanical states $|0,N,0,0\rangle$ or $|0,0,0,N\rangle$ is obtained if the condition $A_1\sqrt{\kappa}|\langle 0,N,0,0|\hat{X}_1|1,m,0,0\rangle| = \pi$ is fulfilled. Once such a transfer is completed, the desired NOON state in Eq. (8) is obtained, provided that the two pulses display the following phase difference:

$$\eta_N^{(2)} - \eta_N^{(1)} = \varphi + \pi/2. \tag{19}$$

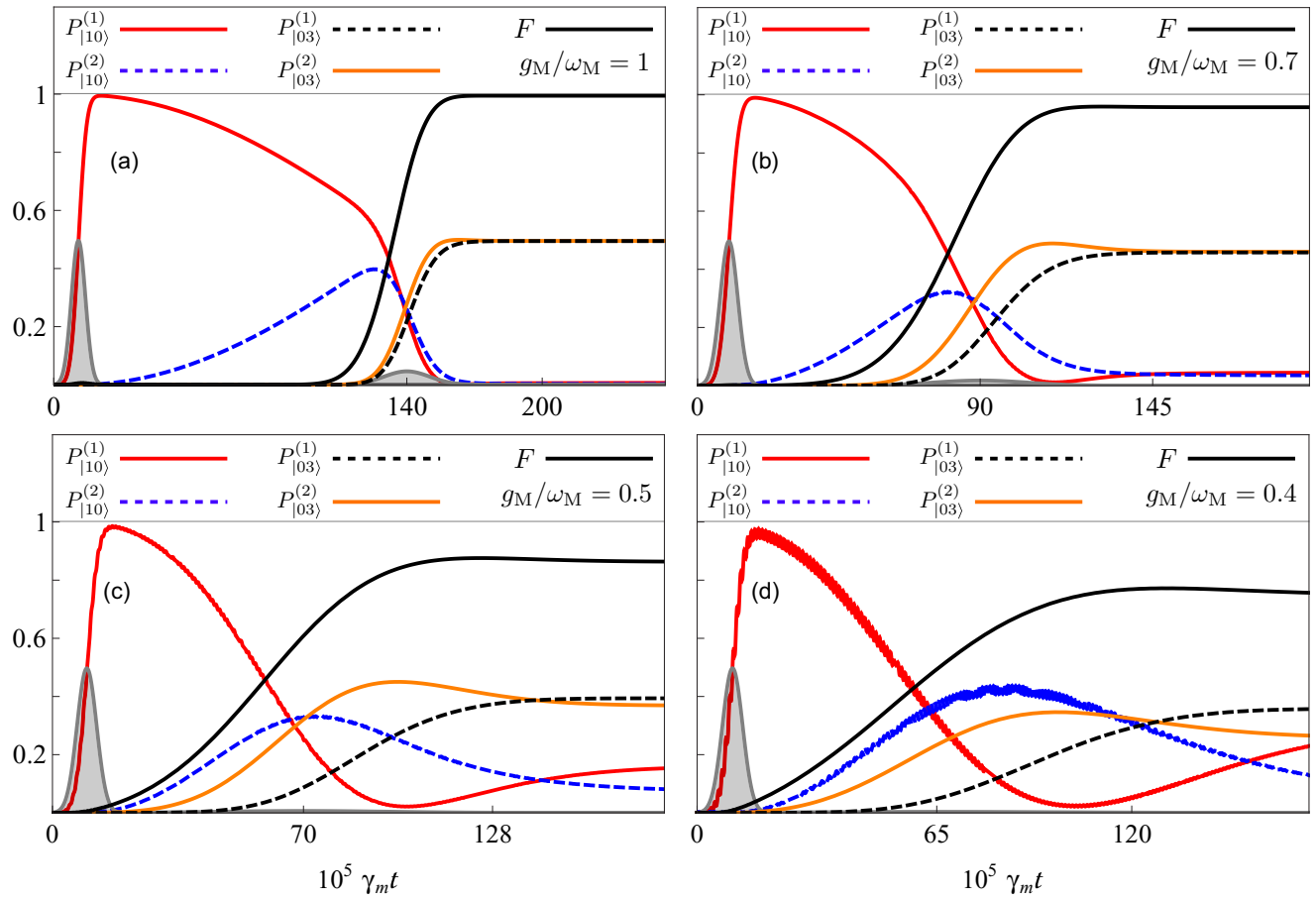

FIG. 4. Time evolution of the occupation probabilities $P^{(1)}_{|1,0\rangle}(t)$, $P^{(2)}_{|1,0\rangle}(t)$, $P^{(1)}_{|0,3\rangle}(t)$, and $P^{(2)}_{|0,3\rangle}(t)$, under the influence of three external π-like Gaussian pulses (gray solid curves). The first pulse, of central frequency ω_0, excites cavity 1. The other two, of central frequency ω_3, have the same arrival time and are sent one to each cavity. The amplitude, phase, and central frequencies of the pulses are chosen in order to generate the target NOON state $|\bar{\psi}\rangle_{\rm mech} = (|3,0\rangle_{\rm mech} - i|0,3\rangle_{\rm mech})/\sqrt{2}$. The time evolution of the fidelity F is also shown. Calculations are displayed for four different coupling mechanical rates: (a) $g_M/\omega_M = 1.0$ ($F_{\rm MAX} = 0.98$), (b) $g_M/\omega_M = 0.7$ ($F_{\rm MAX} = 0.95$), (c) $g_M/\omega_M = 0.5$ ($F_{\rm MAX} = 0.87$), and (d) $g_M/\omega_M = 0.4$ ($F_{\rm MAX} = 0.77$). For both optomechanical systems the other parameters are $\omega_R/\omega_M = 500$, $\kappa/\omega_M = 5 \times 10^{-5}$, $\gamma_m/\kappa = 0.1$, and $g_R/\omega_M = 8 \times 10^{-3}$.

We observe that this protocol can be extended to the implementation of general entangled states. Actually, it is possible to obtain entangled mechanical superpositions of the given

$$|\bar{\Phi}\rangle = \alpha|\Psi\rangle_1 \otimes |0,0\rangle_2 + \beta e^{i\varphi}|0,0\rangle_1 \otimes |\Psi\rangle_2, \qquad (20)$$

which we refer to as the $\Psi OO\Psi$ states, where $|\Psi\rangle_i = \sum_{m=0}^{N} c_m^{(i)}|0,m\rangle_i$ are arbitrary superpositions of one mechanical oscillator. In this case the first step needs no modifications, while the driving Hamltonian in Eq. (16) (second step) includes additional optical pulses ($k > 1$). The effective driving Hamiltonian, describing the jth pulse is

$$\hat{H}^{(1)}_{\rm eff_{(j)}} = \mathcal{E}^{(j)}_{m,m'}(t)e^{i\eta^{(j)}_{m,m'}}|0,m',0,0\rangle\langle 1,m,0,0| + \text{H.c.}, \qquad (21)$$

where the effective amplitudes $\mathcal{E}^{(j)}_{m,m'}(t)$ of the driving fields are given by

$$\mathcal{E}^{(j)}_{m,m'}(t) = \frac{\mathcal{E}_j(t)}{2}\langle 0,m',0,0|\hat{X}_1|1,m,0,0\rangle. \qquad (22)$$

The complete excitation transfer from the ancilla state to the final mechanical superpositions requires the following condition: $A_j\sqrt{\kappa}|\langle 0,m',0,0|\hat{X}_1|1,m,0,0\rangle| = |c^{(1)}_{m'}|\pi$.

In order to correctly describe the quantum dynamics of the system, dissipation induced by its coupling to the environment needs to be considered. We adopt the master equation approach. In the USC regime the description offered by the standard quantum optical master equation breaks down. Following Ref. [64], we exploit a master equation in the dressed state basis, which works for arbitrary optomechanical coupling strengths,

$$\begin{aligned}\dot{\rho}(t) = i[\rho(t),\hat{H}] &+ \sum_{j=1}^{2}\gamma_m^j(n_{\rm th}+1)\mathcal{D}[\hat{C}_j]\rho(t) \\ &+ \sum_{j=1}^{2}\gamma_m^j n_{\rm th}\mathcal{D}[\hat{C}_j^\dagger]\rho(t) + \sum_{j=1}^{2}\kappa_j\mathcal{D}[\hat{a}_j]\rho(t) \\ &+ \sum_{j=1}^{2}\phi_\gamma^j\mathcal{D}[\hat{N}_j]\rho(t), \qquad (23)\end{aligned}$$

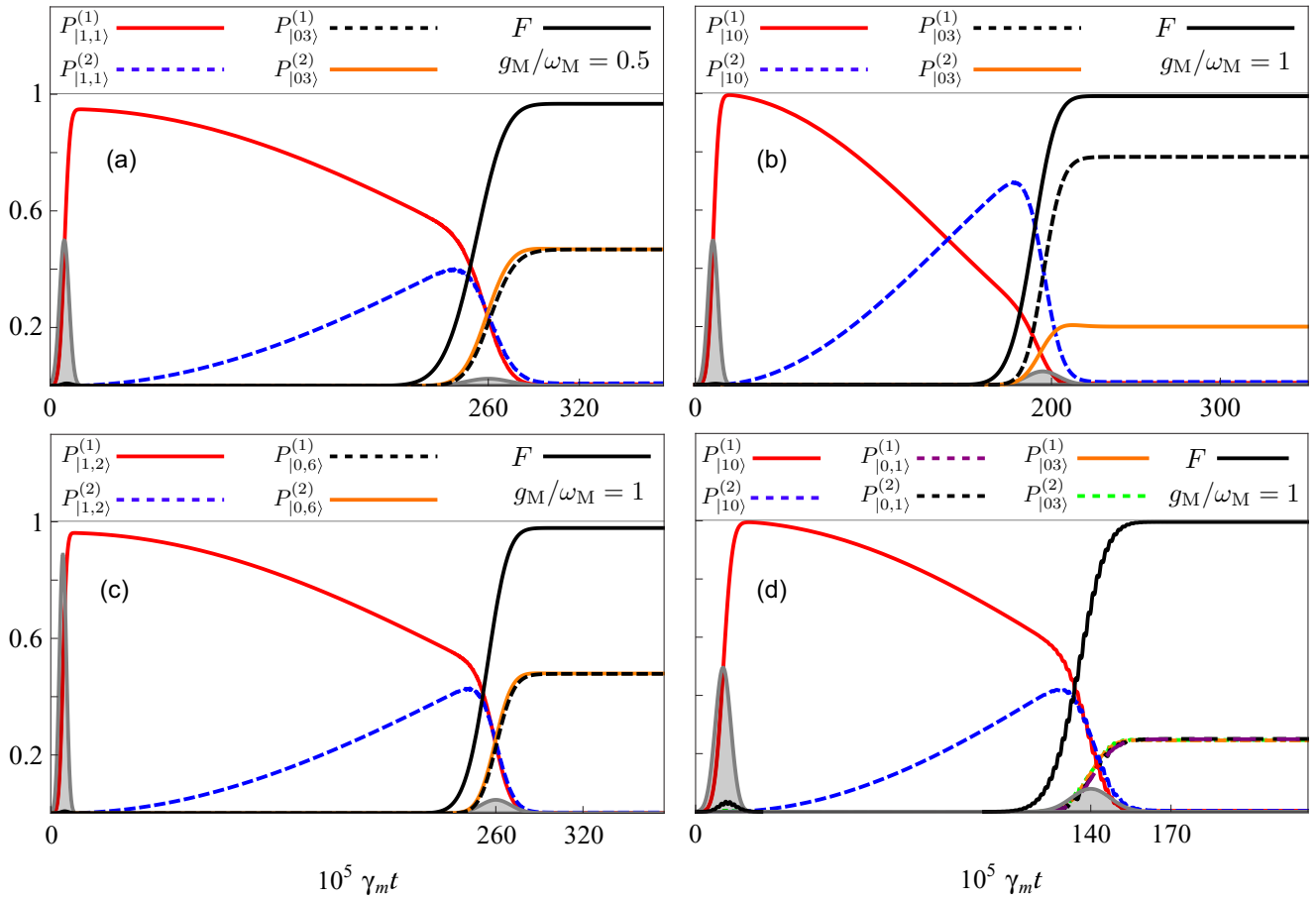

FIG. 5. Examples of time evolution of occupation probabilities and fidelities F for different entangled target states. (a) $|\bar{\psi}\rangle_{\rm mech} = (|3,0\rangle_{\rm mech} - i|0,3\rangle_{\rm mech})/\sqrt{2}$. The dynamics is calculated exploiting the ancilla state $|1,1\rangle$ and for $g_M/\omega_M = 0.5$. The achieved maximal fidelity is $F_{\rm MAX} = 0.963$. (b) Target state: $|\bar{\psi}\rangle_{\rm mech} = (2|3,0\rangle_{\rm mech} - i|0,3\rangle_{\rm mech})/\sqrt{5}$. Here the dynamics is calculated exploiting the ancilla state $|1,0\rangle$ and for $g_M/\omega_M = 1$, with $F_{\rm MAX} = 0.993$. (c) Target state: $|\bar{\psi}\rangle_{\rm mech} = (|6,0\rangle_{\rm mech} - i|0,6\rangle_{\rm mech})/\sqrt{2}$. We calculate the dynamics by starting from the ancilla state $|1,2\rangle$ and for $g_M/\omega_M = 1$, with $F_{\rm MAX} = 0.933$. (d) The target state is the $\bar{\Psi}OO\bar{\Psi}$ state, $|\bar{\Psi}\rangle_{\rm mech} = (|\Psi\rangle_{\rm mech}|0\rangle_{\rm mech} - i|0\rangle_{\rm mech}|\Psi\rangle_{\rm mech})/\sqrt{2}$, where $|\Psi\rangle_{\rm mech} = (|1\rangle_{\rm mech} + |3\rangle_{\rm mech})/\sqrt{2}$. The dynamics is calculated exploiting the ancilla state $|1,0\rangle$ and for $g_M/\omega_M = 1$ and $F_{\rm MAX} = 0.993$ is obtained. For both the optomechanical systems and for all four panels the other parameters are $\omega_R/\omega_M = 500$, $\kappa/\omega_M = 5\times10^{-5}$, $\gamma_m/\kappa = 0.1$, and $g_R/\omega_M = 8\times10^{-3}$.

where $\mathcal{D}[\hat{O}]\hat{\rho} = \frac{1}{2}(2\hat{O}\hat{\rho}\hat{O}^\dagger - \hat{\rho}\hat{O}^\dagger\hat{O} - \hat{O}^\dagger\hat{O}\hat{\rho})$ describes dissipation effects arising from the resonator and the mechanical reservoirs, and $\hat{C}_j = \hat{b}_j - (g_M/\omega_M)\hat{N}_j$ and $\hat{N}_j = \hat{a}_j^\dagger a_j$ are the displacement operator and the photon number operator, respectively. The optical cavity modes are affected by temperature-dependent pure dephasing effects, induced by the optomechanical coupling [64]. Such pure dephasing is taken into account by the last term of Eq. (23), where the coefficients $\phi_\gamma^j = 4K_BT\gamma_m^j g_M/\omega_M^2$ represent the decoherence rates.

Once the target state has been synthesized, there remains the problem of detecting it experimentally, or at least of quantifying its entanglement. The nonclassical nature of this mechanical state can be demonstrated by applying a readout laser on the lower sideband to map the phononic state to a photonic mode and performing an autocorrelation measurement [60,65]. The mechanical excitation is thus coherently mapped onto the external optical cavity $\hat{a}_i^{\rm readout}$. Alternatively, a full quantum tomography of the mechanical state might be carried out. The quantum state can be univocally characterized by employing Wigner tomography. Following the scheme developed by Leibfried *et al.* [66], the reconstruction of the density matrix and the Wigner function of the mechanical quantum state can be obtained. Once the target state is synthesized, the reconstruction mapping can be realized by applying to this state coherent displacements provided by a classical driving field of frequency ω_0 with different amplitudes and phases and then measuring the number-state populations. In analogy with Wigner tomography for trapped ions, a proposal for reconstruction of optomechanical quantum states has been recently presented by Vanner *et al.* [67].

Operating limits

We briefly discuss the requirements that the system parameters and external driving amplitudes have to fulfill for the correct working of this protocol. We observe that Eqs. (13) and (16), beyond the desired resonant contributions shown in Eqs. (14) and (17) respectively, contain also nonresonant (time-oscillating) terms which may induce undesired transitions. In order to face this problem, we can reduce it to a two-state system in the presence of an external pulse. This problem

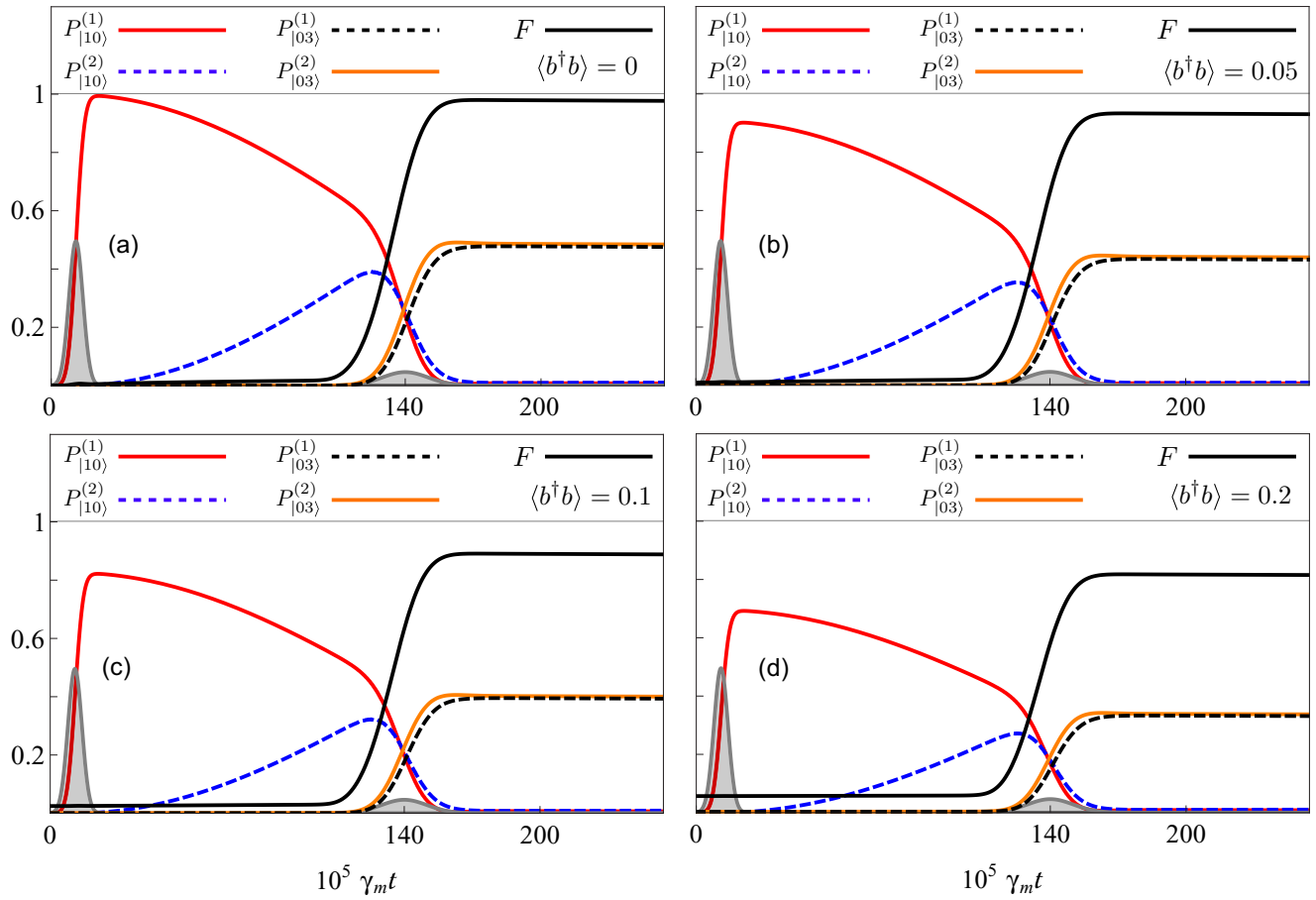

FIG. 6. Time evolution of occupation probabilities $P^{(1)}_{|1,0\rangle}(t)$, $P^{(2)}_{|1,0\rangle}(t)$, $P^{(1)}_{|0,3\rangle}(t)$, and $P^{(2)}_{|0,3\rangle}(t)$, and of the fidelity F during the generation of the target NOON state $|\bar{\psi}\rangle_{\rm mech} = (|3,0\rangle_{\rm mech} - i|0,3\rangle_{\rm mech})/\sqrt{2}$. Here the effects of thermal noise and pure dephasing have been included. In each panel the initial state corresponds to a thermal mechanical state at equilibrium with the mechanical reservoir. Panel (a) has been obtained considering a zero-temperature mechanical reservoir ($\langle \hat{b}^\dagger \hat{b}\rangle = 0$). Panels (b) and (c) have been obtained considering reservoirs with increasing values of thermal noise. The increase of noise determines the lowering of the fidelity. For both the optomechanical systems the other parameters are $\omega_R/\omega_M = 500$, $\kappa/\omega_M = 5 \times 10^{-5}$, $\gamma_m/\kappa = 0.1$, $g_M/\omega_M = 1$, and $g_R/\omega_M = 8 \times 10^{-3}$.

can be easily solved when the central frequency of the pulse is equal to the transition frequency as in Eqs. (14) and (17). However, the general solution for an arbitrary exciting field is much more complicated [68]. It is simpler if the system is subjected to a rectangular exciting pulse. Assuming this pulse shape in Eqs. (13) and (16) [$\mathcal{E}_j(t) = \mathcal{E}$], according to the Rabi problem [68], the probability of undesired adjacent transitions is small if $\mathcal{E}/\omega_M < 1$. Since we are actually considering a Gaussian pulse, we replace the constant amplitude $\mathcal{E}$ with its peak value, thus obtaining: $\sqrt{k} A X_{N\pm1}/(\sqrt{2\pi}\omega_M \Delta) < 1$ where $X_{N\pm1} = \langle 0,N\pm1,0,0|\hat{X}_1|1,m,0,0\rangle$. Since we are using a π pulse for the desired transition between the ancilla states $|1,m\rangle_i$ and the zero-photon mechanical states $|0,N\rangle_i$, the amplitude A is determined by $\sqrt{\kappa} A = \pi/X_N$. We thus obtain $\omega_M \Delta > (X_{N\pm1}/X_N)$. Of course the pulse duration has to be much smaller than the damping rates. Hence the protocol works if the following condition is fulfilled:

$$Q_M \gg \omega_M \Delta > \frac{X_{N\pm1}}{X_N}, \tag{24}$$

where $Q_M = \omega_M/\gamma$ is the mechanical quality factor, and we assume $\gamma > \kappa$. Equation (24) shows that the protocol may fail for ratios $X_{N\pm1}/X_N \gg 1$. In general, a normalized coupling β_0 not much smaller than 1 ensure ratios not much larger than 1.

We complete this section analyzing how the coupling β_0 influences the matrix elements. The matrix elements in Eqs. (15) and (18) can be easily derived using Eqs. (4)–(6):

$$\langle 0,N,0,0|\hat{X}_1|1,m,0,0\rangle = \sum_{k=0}^{m} \frac{\sqrt{m!\,N!}}{k!(m-k)!(N-m-k)!}\,\beta_0^k\, d_{N-m-k}. \tag{25}$$

Figure 3 shows the transition matrix elements $\langle 0,N,0,0|\hat{X}_1|1,m,0,0\rangle$ as a function of the vibrational quantum number N for different values of the optomechanical coupling rates g_M/ω_M and considering the cases in which the ancilla state has, respectively, phonon number $m = 0$, 1, 2, and 3 . We note that in order to create NOON states with increasing N, higher values of g_M/ω_M are required, because if the coupling rate is not strong enough, i.e., the system is not in the optomechanical USC regime, only the first mechanical states can be coupled. In order to synthesize the target state, the protocol requires that both the transitions $|0,0,0,0\rangle \leftrightarrow |1,m,0,0\rangle$ and $|1,m,0,0\rangle \leftrightarrow |0,N,0,0\rangle$ are possible; namely, Eqs. (15)

and (18), $\langle 0,0,0,0|\hat{X}_1|1,m,0,0\rangle$ and $\langle 0,N,0,0|\hat{X}_1|1,m,0,0\rangle$, have to be significantly different from zero. Figures 3(a)–3(d) clearly show that, if the coupling rate g_M/ω_M is too low (blue circles), this last condition is not fulfilled. In fact, for every fixed value of the ancilla state phonon number m the only relevant transition matrix elements $\langle 0,N,0,0|\hat{X}_1|1,m,0,0\rangle$ are those with $m = N$. Specifically, when $m = 0$ and for low values of the optomechanical coupling rate only the first mechanical states can be coupled. On the other hand, when $m > 0$ the result is that $\langle 0,0,0,0|\hat{X}_1|1,m,0,0\rangle$ always displays a very small value and this implies that the ancilla state cannot be efficiently populated.

IV. NUMERICAL RESULTS

In this article, unless otherwise stated, we consider the following system parameters for the two identical optomechanical systems:$\omega_R/\omega_M = 500$, $g_M/\omega_M = 1$, $\kappa/\omega_M = 5\times 10^{-5}$, $\gamma_m/\kappa = 0.1$, and $g_R/\omega_M = 8\times 10^{-3}$. We use $P^{(1)}_{|n,m\rangle}(t) = \langle n,m,0,0|\rho(t)|n,m,0,0\rangle$ and $P^{(2)}_{|n,m\rangle}(t) = \langle 0,0,n,m|\rho(t)|0,0,n,m\rangle$ to indicate, respectively, the time evolution of the occupation probabilities for the states of system 1 and system 2.

In Figs. 4 and 5, we present numerical calculations carried out considering the system at $T = 0$ K, i.e., in the absence of thermal noise. Figure 4 displays the time evolution of occupation probabilities $P^{(1)}_{|1,0\rangle}(t)$, $P^{(1)}_{|0,3\rangle}(t)$, $P^{(2)}_{|1,0\rangle}(t)$, and $P^{(2)}_{|0,3\rangle}(t)$ under the influence of three external π pulses of central frequency ω_0 and ω_3 chosen in order to generate the target NOON state $|\bar{\psi}\rangle_{\rm mech} = \frac{1}{\sqrt{2}}(|3,0\rangle_{\rm mech} - i|0,3\rangle_{\rm mech})$ for optomechanical coupling rates $g_M/\omega_M = 1.0$ (a), $g_M/\omega_M = 0.7$ (b), $g_M/\omega_M = 0.5$ (c), and $g_M/\omega_M = 0.4$ (d). Following the protocol described in Sec. III, in order to synthesize the mechanical NOON state $|\bar{\psi}\rangle_{\rm mech} = \frac{1}{\sqrt{2}}(|3,0\rangle_{\rm mech} - i|0,3\rangle_{\rm mech})$, a π pulse (first gray solid curve) of central frequency ω_0 was sent to system 1 in order to completely populate the ancilla state $|1,0\rangle_1$: $P^{(1)}_{|1,0\rangle}(t) \simeq 1$. Then, at the instant of time $t^* = \pi/4g_R$ we sent two additional π pulses of central frequency ω_3 (second gray solid curve) to both systems in order to depopulate the superposition $|\psi(t)\rangle$ state in Eq. (9), towards pure mechanical states $|0,3\rangle_1$ and $|0,3\rangle_2$, so that $P^{(1)}_{|0,3\rangle}(t) = P^{(2)}_{|0,3\rangle}(t) = 0.5$. In order to quantify the correspondence between the achieved and the target states, we exploit the fidelity. We observe that when g_M/ω_M decreases, the transition matrix elements between the intermediate ancilla state and the mechanical states decrease contributing to a decrease of the occupation probabilities. The fidelities $F = \sqrt{\langle\bar{\psi}|\rho|\bar{\psi}\rangle}$ between the desired target states $|\bar{\psi}\rangle$ and the density matrices ρ of the synthesized states are, from Figs. 4(a) to 4(d), $F = 0.98$, 0.95, 0.87, and 0.77. This shows that, choosing the state $|1,0\rangle_1$ as the ancilla state, the protocol is less efficient for low values of the mechanical coupling rate g_M/ω_M.

In Fig. 5(a) we show the dynamics describing the synthesis of the same mechanical NOON state $|\bar{\psi}\rangle_{\rm mech} = \frac{1}{\sqrt{2}}(|3,0\rangle_{\rm mech} - i|0,3\rangle_{\rm mech})$ as in Fig. 4(c), choosing as the ancilla state the state $|1,1\rangle_1$ rather than $|1,0\rangle_1$. Numerical results show that, for the same value of the optomechanical coupling rate ($g_M/\omega_M = 0.5$), the choice of a higher-energy ancilla state leads to an improvement in the synthesis of the target state, as confirmed by the higher value of the fidelity [$F = 0.963$ compared with $F = 0.87$ in Fig. 4(c)]. Figure 5(b) shows the dynamics leading to the synthesis of the target quantum NOON state $|\bar{\psi}\rangle_{\rm mech} = \frac{2}{\sqrt{5}}|3,0\rangle_{\rm mech} - \frac{i}{\sqrt{5}}|0,3\rangle_{\rm mech}$. In this case the second Gaussian pulse must be sent at the instant of time $t^* = g_R^{-1}\arctan(1/2)$. Figure 5(c) shows how it is possible to apply the here present protocol to realize mechanical NOON states with a higher mechanical Fock-state number N. Specifically, it displays the realization of the NOON state $|\bar{\psi}\rangle_{\rm mech} = \frac{1}{\sqrt{2}}(|6,0\rangle_{\rm mech} - i|0,6\rangle_{\rm mech})$ by choosing the state $|1,2\rangle_1$ as the ancilla state. From Fig. 3(d), it would seem more convenient to use the ancilla state $|1,3\rangle_1$, being $\langle 0,6,0,0|\hat{X}_1|1,3,0,0\rangle > \langle 0,6,0,0|\hat{X}_1|1,2,0,0\rangle$. However, numerical calculations show that a choice of the ancilla state $|1,3\rangle_1$ implies a longer time training which could lower the probabilities of synthesizing the state in the presence of thermal noise. Finally, in Fig. 5(d) we realize the target quantum state $|\bar{\Psi}\rangle_{\rm mech} = \frac{1}{\sqrt{2}}[\frac{1}{\sqrt{2}}(|1,0\rangle_{\rm mech} + |3,0\rangle_{\rm mech}) - i\frac{1}{\sqrt{2}}(|0,1\rangle_{\rm mech} + |0,3\rangle_{\rm mech})]$, showing how the here proposed protocol can be effectively used to synthesize, with high

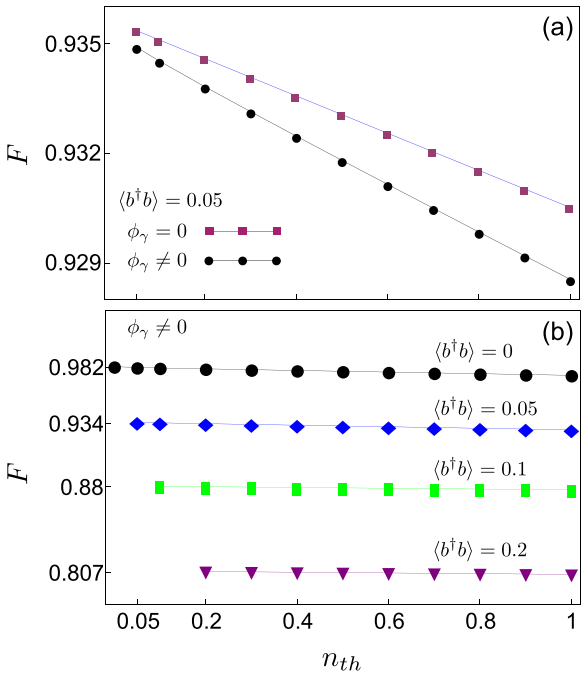

FIG. 7. The effects of thermal noise on the calculation of the fidelities when we apply the protocol for the synthesis of the target quantum NOON state $|\bar{\psi}\rangle_{\rm mech} = (|3,0\rangle_{\rm mech} - i|0,3\rangle_{\rm mech})/\sqrt{2}$. (a) Trend of the fidelity as a function of $n_{\rm th}$ when the system is initially prepared in a thermal state with the mean occupation number $\langle\hat{b}^\dagger\hat{b}\rangle = 0.05$, in the presence and in the absence of pure dephasing ϕ_γ. The fidelity decreases faster when the effects of dephasing are taken into account. (b) Trend of fidelities as a function of $n_{\rm th}$ when the system is initially prepared in different thermal states with increasing mean occupation number $\langle\hat{b}^\dagger\hat{b}\rangle$ and in the presence of pure dephasing ϕ_γ. For both optomechanical systems the other parameters are $\omega_R/\omega_M = 500, \kappa/\omega_M = 5\times 10^{-5}, \gamma_m/\kappa = 0.1, g_M/\omega_M = 1$, and $g_R/\omega_M = 8\times 10^{-3}$.

fidelity, more general entangled mechanical superposition $\Psi O O \Psi$ states.

In real optomechanical systems, ground-state cooling is never complete and the interaction with a finite-temperature reservoir also has to be taken into account. In order to describe the influence of the dissipation and decoherence processes, we solve numerically the dressed master equation, Eq. (23). Figure 6 shows the effects of thermal noise on the synthesis of the state $|\bar{\psi}\rangle_{\rm mech} = \frac{1}{\sqrt{2}}(|3,0\rangle_{\rm mech} - i|0,3\rangle_{\rm mech})$, when the system is initially prepared in a thermal state with mean occupation numbers $\langle \hat{b}^\dagger \hat{b}\rangle = 0$ (a), 0.05 (b), 0.1 (c), and 0.2 (d). Here we consider the case where the mechanical system is in thermal equilibrium with the reservoir. The effects of the pure dephasing ϕ_γ induced by the optomechanical coupling, described in the last term of Eq. (23), are also considered. It can be observed that the effects of thermal noise can be relevant as confirmed by the lower values of the fidelities obtained as the temperature increases. In Fig. 7 we consider the effects of thermal noise on the calculation of the fidelities when we apply the protocol for the synthesis of the target quantum NOON state $|\bar{\psi}\rangle_{\rm mech} = \frac{1}{\sqrt{2}}(|3,0\rangle_{\rm mech} - i|0,3\rangle_{\rm mech})$. Specifically, Fig. 7(a) shows the trend of the fidelity as a function of the mechanical reservoir noise $n_{\rm th}$ when the system is initially prepared in a thermal state with a small mean occupation number $\langle \hat{b}^\dagger \hat{b}\rangle = 0.05$. Calculations have been performed both in the presence and in the absence of pure dephasing ϕ_γ. It can be observed that, for increasing value of temperature, the fidelity decreases faster when the effects of dephasing are taken into account [see Eq. (23)]. Finally, in Fig. 7(b) we show the trend of fidelities as a function of the mean occupation number $n_{\rm th}$ of the mechanical reservoir when the system is initially prepared in different thermal states with increasing mean occupation number $\langle \hat{b}^\dagger \hat{b}\rangle = 0$, 0.05, 0.1, and 0.2 and in presence of pure dephasing ϕ_γ.

V. CONCLUSION

We presented a strategy for the preparation of the maximally entangled mechanical NOON states in optomechanical systems in a completely controlled and deterministic manner. In the optomechanical USC regime, when the coupling strength becomes a significant fraction of the mechanical frequency, we have shown that NOON mechanical states with quite high Fock states can be deterministically obtained within a few-step protocol. The framework presented here provides an example of how the USC regime can favor the generation of entangled mechanical quantum states. Such states can be viewed as a benchmark for multimode state preparation and coherent control capabilities. Moreover they play an important role in quantum metrology and sensing [69,70]. The generation of mechanical NOON states offers a route towards fundamental tests of quantum mechanics, such as the effects of decoherence on many-particle entanglement [71,72] and the quantum-classical crossover in a parameter regime beyond microscopic sizes and masses [73].

One key feature of the protocol presented here is that it consists of a few operations independently of the specific Fock state in the target NOON states. In the ideal case the system starts in its ground state. The protocol starts sending a π pulse to one optical resonator with central frequency equal to the frequency difference between an ancilla state $|1,j\rangle$ and the ground state. Then, the system is subject to a spontaneous Rabi-like oscillation able to partly transfer the excitation to the second optomechanical system. The final step consists of sending simultaneously two additional π-like Gaussian optical pulses, one at each optical resonator, with a central frequency corresponding to the frequency difference between the ancilla state and the final desired mechanical Fock state.

The operating range of this protocol has been carefully analyzed. We tested the efficiency and robustness of this protocol by applying it to different situations, calculating fidelities in the presence of decoherence and thermal noise, and including the effects of dephasing and imperfect cooling. This approach can also be exploited for obtaining more general entangled states. For example, we have shown that, within a two-step operation, $\Psi O O \Psi$ states can be synthesized. These many-body entangled states realize the situation where one of the two resonators is in an arbitrary superposition of Fock states, with the other in its ground state and vice versa.

[1] K. Stannigel, P. Komar, S. J. M. Habraken, S. D. Bennett, M. D. Lukin, P. Zoller, and P. Rabl, Optomechanical Quantum Information Processing with Photons and Phonons, Phys. Rev. Lett. **109**, 013603 (2012).

[2] M. Aspelmeyer, T. J. Kippenberg, and F. Marquardt, Cavity optomechanics, Rev. Mod. Phys. **86**, 1391 (2014).

[3] P. Meystre, A short walk through quantum optomechanics, Ann. Phys. (Berlin) **525**, 215 (2013).

[4] Y.-D. Wang and A. A. Clerk, Using Interference for High Fidelity Quantum State Transfer in Optomechanics, Phys. Rev. Lett. **108**, 153603 (2012).

[5] S. A. McGee, D. Meiser, C. A. Regal, K. W. Lehnert, and M. J. Holland, Mechanical resonators for storage and transfer of electrical and optical quantum states, Phys. Rev. A **87**, 053818 (2013).

[6] T. A. Palomaki, J. W. Harlow, J. D. Teufel, R. W. Simmonds, and K. W. Lehnert, Coherent state transfer between itinerant microwave fields and a mechanical oscillator, Nature (London) **495**, 210 (2013).

[7] Eyob A. Sete and H. Eleuch, High-efficiency quantum state transfer and quantum memory using a mechanical oscillator, Phys. Rev. A **91**, 032309 (2015).

[8] M. Aspelmeyer, S. Gröblacher, Klemens Hammerer, and N. Kiesel, Quantum optomechanicsthrowing a glance, J. Opt. Soc. Am. B **27**, A189 (2010).

[9] T. J. Kippenberg and K. J. Vahala, Cavity optomechanics: Back-action at the mesoscale, Science **321**, 1172 (2008).

[10] I. Favero and K. Karrai, Optomechanics of deformable optical cavities, Nat. Photonics **3**, 201 (2009).

[11] F. Marquardt and S. M. Girvin, Optomechanics, Physics **2**, 40 (2009).

[12] D. Van Thourhout and J. Roels, Optomechanical device actuation through the optical gradient force, Nat. Photonics **4**, 211 (2010).

[13] M. Poot and H. S. J. van der Zant, Mechanical systems in the quantum regime, Phys. Rep. **511**, 273 (2012).
[14] X. Y. Lü, Y. Wu, J. R. Johansson, H. Jing, J. Zhang, and F. Nori, Squeezed Optomechanics with Phase-Matched Amplification and Dissipation, Phys. Phys. Lett. **114**, 093602 (2015).
[15] G. Vacanti, M. Paternostro, G. M. Palma, M. S. Kim, and V. Vedral, Nonclassicality of optomechanical devices in experimentally realistic operating regimes, Phys. Rev. A **88**, 013851 (2013).
[16] S. Bose, K. Jacobs, and P. L. Knight, Scheme to probe the decoherence of a macroscopic object, Phys. Rev. A **59**, 3204 (1999).
[17] W. Marshall, C. Simon, R. Penrose, and D. Bouwmeester, Towards Quantum Superpositions of a Mirror, Phys. Rev. Lett. **91**, 130401 (2003).
[18] B. Pepper, R. Ghobadi, E. Jeffrey, C. Simon, and D. Bouwmeester, Optomechanical Superpositions via Nested Interferometry, Phys. Rev. Lett. **109**, 023601 (2012).
[19] S. P. Vyatchanin and A. B. Matsko, Quantum limit on force measurements, JETP **77**, 218 (1993).
[20] C. Fabre, M. Pinard, S. Bourzeix, A. Heidmann, E. Giacobino, and S. Reynaud, Quantum-noise reduction using a cavity with a movable mirror, Phys. Rev. A **49**, 1337 (1994).
[21] S. Mancini and P. Tombesi, Quantum noise reduction by radiation pressure, Phys. Rev. A **49**, 4055 (1994).
[22] P. Verlot, A. Tavernarakis, C. Molinelli, A. Kuhn, T. Antoni, S. Gras, T. Briant, P. F. Cohadon, A. Heidmann, and L. Pinard, Towards the experimental demonstration of quantum radiation pressure noise, C. R. Physs **12**, 826 (2011).
[23] D. W. C. Brooks, T. Botter, S. Schreppler, T. P. Purdy, N. Brahms, and D. M. Stamper-Kurn, Non-classical light generated by quantum-noise-driven cavity optomechanics, Nature (London) **488**, 476 (2012).
[24] A. H. Safavi-Naeini, S. Gröblacher, J. T. Hill, J. Chan, M. Aspelmeyer, and O. Painter, Squeezed light from a silicon micromechanical resonator, Nature (London) **500**, 185 (2013).
[25] A. D. O'Connell, M. Hofheinz, M. Ansmann, R. C. Bialczak, M. Lenander, E. Lucero, D. Neeley, M. Sank, H. Wang, and M. Weides, Quantum ground state and single-phonon control of a mechanical resonator, Nature (London) **464**, 697 (2010).
[26] P. F. Cohadon, A. Heidmann, and M. Pinard, Cooling of a Mirror by Radiation Pressure, Phys. Rev. Lett. **83**, 3174 (1999).
[27] O. Arcizet, P. F. Cohadon, T. Briant, M. Pinard, and Antoine Heidmann, Radiation-pressure cooling and optomechanical instability of a micromirror, Nature (London) **444**, 71 (2006).
[28] A. Schliesser, P. Del'Haye, N. Nooshi, K. J. Vahala, and T. J. Kippenberg, Radiation Pressure Cooling of a Micromechanical Oscillator using Dynamical Backaction, Phys. Rev. Lett. **97**, 243905 (2006).
[29] X.-w. Xu, H. Wang, J. Zhang, and Y.-x. Liu, Engineering of nonclassical motional states in optomechanical systems, Phys. Rev. A **88**, 063819 (2013).
[30] C. K. Law and J. H. Eberly, Arbitrary Control of a Quantum Electromagnetic Field, Phys. Rev. Lett. **76**, 1055 (1996).
[31] S. Bose, K. Jacobs, and P. L. Knight, Preparation of nonclassical states in cavities with a moving mirror, Phys. Rev. A **56**, 4175 (1997).
[32] S. Deleglise, I. Dotsenko, C. Sayrin, J. Bernu, M. Brune, J. M. Raimond, and S. Haroche, Reconstruction of non-classical cavity field states with snapshots of their decoherence, Nature (London) **455**, 510 (2008).
[33] D. Kleckner, I. Pikovski, E. Jeffrey, L. Ament, E. Eliel, J. Van Den Brink, and D. Bouwmeester, Creating and verifying a quantum superposition in a micro-optomechanical system, New J. Phys. **10**, 095020 (2008).
[34] M. Hofheinz, H. Wang, M. Ansmann, R. C. Bialczak, E. Lucero, M. Neeley, A. D. O'Connell, D. Sank, J. Wenner, and J. M. Martinis, Synthesizing arbitrary quantum states in a superconducting resonator, Nature (London) **459**, 546 (2009).
[35] S. A. Gardiner, J. I. Cirac, and P. Zoller, Nonclassical states and measurement of general motional observables of a trapped ion, Phys. Rev. A **55**, 1683 (1997).
[36] B. Kneer and C. K. Law, Preparation of arbitrary entangled quantum states of a trapped ion, Phys. Rev. A **57**, 2096 (1998).
[37] L. F. Wei, Y.-x. Liu, and F. Nori, Engineering quantum pure states of a trapped cold ion beyond the Lamb-Dicke limit, Phys. Rev. A **70**, 063801 (2004).
[38] L. Garziano, R. Stassi, V. Macrí, S. Savasta, and O. Di Stefano, Single-step arbitrary control of mechanical quantum states in ultrastrong optomechanics, Phys. Rev. A **91**, 023809 (2015).
[39] X. W. Xu, Y. J. Zhao, and Y. X. Liu, Entangled-state engineering of vibrational modes in a multimembrane optomechanical system, Phys. Rev. A **88**, 022325 (2013).
[40] A. Nunnenkamp, K. Børkje, and S. M. Girvin, Single-Photon Optomechanics, Phys. Rev. Lett. **107**, 063602 (2011).
[41] A. J. Rimberg, M. P. Blencowe, A. D. Armour, and P. D. Nation, A cavity-Cooper pair transistor scheme for investigating quantum optomechanics in the ultra-strong coupling regime, New J. Phys. **16**, 055008 (2014).
[42] T. T. Heikkilä, F. Massel, J. Tuorila, R. Khan, and M. A. Sillanpää, Enhancing Optomechanical Coupling via the Josephson Effect, Phys. Rev. Lett. **112**, 203603 (2014).
[43] T. Niemczyk, F. Deppe, H. Huebl, E. P. Menzel, F. Hocke, M. J. Schwarz, J. J. García-Ripoll, D. Zueco, T. Hümmer, and E. Solano, Circuit quantum electrodynamics in the ultrastrong-coupling regime, Nat. Phys. **6**, 772 (2010).
[44] A. Ridolfo, M. Leib, S. Savasta, and M. J. Hartmann, Photon Blockade in the Ultrastrong Coupling Regime, Phys. Rev. Lett. **109**, 193602 (2012).
[45] S. Ashhab and F. Nori, Qubit-oscillator systems in the ultrastrong-coupling regime and their potential for preparing nonclassical states, Phys. Rev. A **81**, 042311 (2010).
[46] A. Ridolfo, S. Savasta, and M. J. Hartmann, Nonclassical Radiation from Thermal Cavities in the Ultrastrong Coupling Regime, Phys. Rev. Lett. **110**, 163601 (2013).
[47] L. Garziano, A. Ridolfo, R. Stassi, O. Di Stefano, and S. Savasta, Switching on and off of ultrastrong light-matter interaction: Photon statistics of quantum vacuum radiation, Phys. Rev. A **88**, 063829 (2013).
[48] J. F. Huang and C. K. Law, Photon emission via vacuum-dressed intermediate states under ultrastrong coupling, Phys. Rev. A **89**, 033827 (2014).
[49] L. Garziano, R. Stassi, A. Ridolfo, O. Di Stefano, and S. Savasta, Vacuum-induced symmetry breaking in a superconducting quantum circuit, Phys. Rev. A **90**, 043817 (2014).
[50] S. Mancini, V. I. Man'ko, and P. Tombesi, Ponderomotive control of quantum macroscopic coherence, Phys. Rev. A **55**, 3042 (1997).

[51] J. Q. Liao, C. K. Law, L. M. Kuang, and F. Nori, Enhancement of mechanical effects of single photons in modulated two-mode optomechanics, Phys. Rev. A **92**, 013822 (2015).

[52] M. Paternostro, D. Vitali, S. Gigan, M. S. Kim, C. Brukner, J. Eisert, and M. Aspelmeyer, Creating and Probing Multipartite Macroscopic Entanglement with Light, Phys. Rev. Lett. **99**, 250401 (2007).

[53] D. Vitali, S. Gigan, A. Ferreira, H. R. Böhm, P. Tombesi, A. Guerreiro, V. Vedral, A. Zeilinger, and M. Aspelmeyer, Optomechanical Entanglement Between a Movable Mirror and a Cavity Field, Phys. Rev. Lett. **98**, 030405 (2007).

[54] A. Mari and J. Eisert, Opto-and electro-mechanical entanglement improved by modulation, New J. Phys. **14**, 075014 (2012).

[55] J. Zhang, K. Peng, and S. L. Braunstein, Quantum-state transfer from light to macroscopic oscillators, Phys. Rev. A **68**, 013808 (2003).

[56] G. Vacanti, M. Paternostro, G. M. Palma, and V. Vedral, Optomechanical to mechanical entanglement transformation, New. J. Phys. **10**, 095014 (2008).

[57] B. C. Sanders, Quantum dynamics of the nonlinear rotator and the effects of continual spin measurement, Phys. Rev. A **40**, 2417 (1989).

[58] A. N. Boto, P. Kok, D. S. Abrams, S. L. Braunstein, C. P. Williams, and J. P. Dowling, Quantum Interferometric Optical Lithography: Exploiting Entanglement to Beat the Diffraction Limit, Phys. Rev. Lett. **85**, 2733 (2000).

[59] X. X. Ren, H. K. Li, M. Y. Yan, Y. C. Liu, Y. F. Xiao, and Q. Gong, Single-photon transport and mechanical NOON-state generation in microcavity optomechanics, Phys. Rev. A **87**, 033807 (2013).

[60] H. Flayac and V. Savona, Heralded Preparation and Readout of Entangled Phonons in a Photonic Crystal Cavity, Phys. Rev. Lett. **113**, 143603 (2014).

[61] G. De Chiara, M. Paternostro, and G. M. Palma, Entanglement detection in hybrid optomechanical systems, Phys. Rev. A **83**, 052324 (2011).

[62] Eyob A. Sete, Hichem Eleuch, and C. H. Raymond Ooi, Light-to-matter entanglement transfer in optomechanics, J. Opt. Soc. Am. B **31**, 2821 (2014).

[63] J. Q. Liao, Q. Q. Wu, and F. Nori, Entangling two macroscopic mechanical mirrors in a two-cavity optomechanical system, Phys. Rev. A **89**, 014302 (2014).

[64] D. Hu, S. Y. Huang, J. Q. Liao, L. Tian, and H. S. Goan, Quantum coherence in ultrastrong optomechanics, Phys. Rev. A **91**, 013812 (2015).

[65] C. Galland, N. Sangouard, N. Piro, N. Gisin, and T. J. Kippenberg, Heralded Single-Phonon Preparation, Storage, and Readout in Cavity Optomechanics, Phys. Rev. Lett. **112**, 143602 (2014).

[66] D. Leibfried, D. M. Meekhof, B. E. King, C. H. Monroe, W. M. Itano, and D. J. Wineland, Experimental Determination of the Motional Quantum State of a Trapped Atom, Phys. Rev. Lett. **77**, 4281 (1996).

[67] M. R. Vanner, I. Pikovski, G. D. Cole, M. S. Kim, Č. Brukner, K. Hammerer, G. J. Milburn, and M. Aspelmeyer, Pulsed quantum optomechanics, Proc. Nat. Acad. Sci. USA **108**, 16182 (2011).

[68] L. Mandel and E. Wolf, *Optical Coherence and Quantum Optics* (Cambridge University Press, Cambridge, UK, 1995).

[69] H. Lee, P. Kok, and J. P. Dowling, A quantum rosetta stone for interferometry, J. Mod. Opt. **49**, 2325 (2002).

[70] M. W. Mitchell, J. S. Lundeen, and A. M. Steinberg, Super-resolving phase measurements with a multiphoton entangled state, Nature (London) **429**, 161 (2004).

[71] L. Aolita, R. Chaves, D. Cavalcanti, A. Acín, and L. Davidovich, Scaling Laws for the Decay of Multiqubit Entanglement, Phys. Rev. Lett. **100**, 080501 (2008).

[72] H. S. Eisenberg, G. Khoury, G. A. Durkin, C. Simon, and D. Bouwmeester, Quantum Entanglement of a Large Number of Photons, Phys. Rev. Lett. **93**, 193901 (2004).

[73] S. L. Adler and A. Bassi, Is quantum theory exact?, Science **325**, 275 (2009).